Iraqi J. Laser, Part B, Vol. 13, pp.23-31 (2014)

IRAQI JOURNAL OF LASER

Photoacoustic Imaging for Tumor Detection: An in vitro Simulation Study

Arwa A. Moosa and **Mohammed A. Hussain**

Department of Laser and Optoelectronics Engineering, Al-Nahrain University, Baghdad, Iraq

(Received 30 January 2014; accepted 2 September 2014)

Abstract: Photoacoustic is a unique imaging method that combines the absorption contrast of light or radio frequency waves with ultrasound resolution. When the deposition of this energy is sufficiently short, a thermo-elastic expansion takes place whereby acoustic waves are generated. These waves can be recorded and stored to construct an image. This work presents experimental procedure of laser photoacoustic two dimensional imaging to detect tumor embedded within normal tissue. The experimental work is accomplished using phantoms that are sandwiched from fish heart or blood sac (simulating a tumor) 1-14mm mean diameter embedded within chicken breast to simulate a real tissue. Nd: YAG laser of 1.064μm and 532nm wavelengths, 10ns pulse duration, 445mJ pulse energy has been used to induce the acoustic wave signal in these targets. The acoustic signal is then filtered and analyzed to construct the target image. The analysis of experimental data and image construction has been accomplished using matlab software. The measurement analysis showed reasonable agreement between the estimated object dimension and the actual object size. The error in fish heart object dimension ranged from -14% to +9%, and the maximum error in Blood sac object dimension was -55%. The object dimensional error increased to -92% when the laser spot was magnified from 2mm to 45mm (to cover the phantom area) as the energy density decreases significantly.

Introduction

Photo Acoustic Imaging (PAI) is a general name that refers to a collection of non-invasive imaging techniques, which are used to get pictures of biological tissues and their internal structures [1].

Photoacoustic imaging is based on the photoacoustic effect that converts optical energy into acoustic energy. This phenomenon appears whenever a tissue is exposed to a short-pulsed laser beam in the nanosecond time scale. As a consequence, some of the light is absorbed; most of the absorbed energy will transform into heat. Because of thermoelastic expansion, this heat is then converted to mechanical stress. The pressure rise travels in the tissue like a broadband ultrasonic wave, this wave is generally called photoacoustic wave. If this wave is detected by an ultrasonic transducer, it is possible to use the information that it provides to form an image of the photoacoustic source [1-2] as shown in figure 1.

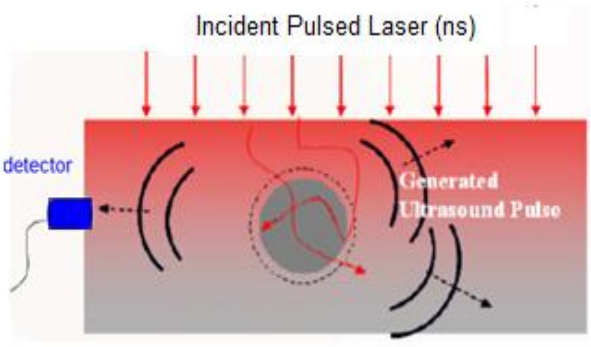

Fig. (1): Schematic of photoacoustic effect, adapted from [3]

The selection of the correct optical wavelength is extremely important in photoacoustic imaging [4]. PA imaging usually uses light in the non-ionizing visible or near-infrared (NIR) parts of the spectrum, for these wavelength ranges, and for light intensities below exposure safety limits, heat deposition is the dominant mechanism for the generation of acoustic pulses [5]. Due to the strong optical scattering effect in biological tissues that enhances the effective optical absorption, light intensity, and hence photoacoustic strength, decreases with depth approximately exponentially, with a decay constant of a few millimeters [1]. To reach deeper tissue structures, NIR is a better excitation source since it has a low water absorption coefficient and a relatively low scattering coefficient in biological tissues and can, consequently, provide deeper penetration (a few centimeters in tissue up to ~7 cm [6-7]) [3]. When a pulsed beam of light strikes a medium, the medium emits sound waves that vary in intensity with the amount of light absorbed. If these sound waves can be detected, a reconstruction of the medium becomes possible. Since the wavelength of light used can be altered to fit the absorption spectra within the medium, this adaptable technique has many uses, including accurate detection of some cancers, and possible treatment [8].

Types of PA imaging systems:

PA Microscopy (PAM): Uses spherically focused ultrasonic transducers with 2D point by point scanning to localize the PA sources in linear or sector scans, and then reconstruct the image directly from the measured data set. Its imaging depth is limited by the ultrasonic attenuation. Detects changes in oxygenated / deoxygenated Hb in small vessels, images skin melanoma [9]. Photoacoustic / Thermoacoustic / Optoacoustic Tomography (PAT/TAT/OAT): Images complicated structures by using a pulse laser as a pumping source to irradiate a medium. PAT makes use of PA signals measured at various locations around the subject understudy. A typical PAT system uses an unfocused (wideband) ultrasound detector, usually in a circular or spherical fashion [9]. Detects brain lesion, monitors hemodynamics, diagnoses breast cancer [10-12].

Photoacoustic imaging has been developed rapidly in the past decade, with applications explored in cancer detection (preferred in breast cancer, because it can be used to determine the stage of the cancer; by using different wavelengths) , imaging vascular structures in tissue, mapped rat brain structures with and without lesion , monitoring the temperature distribution in tissues noninvasively. This is in addition to its ability in diagnosis, therapy planning and monitoring of treatment outcome for cancer, cardiovascular disease, and other pathologies [8, 13-15].

PAI has the advantages of being non-ionizing radiation, its ability to detect cancer at early stages and with a high spatial resolution in sub- microns and in breast cancer detection use with requires no or mild breast compression which can make the process more comfortable for the patients [13]. However the most important challenges in PAI for in vivo animal study and eventual clinical translation are the limited penetration depth of the source light (The effective penetration depth of the light is determined by the scattering and absorption coefficients of the tissues). The PA imaging depth is mainly limited by the attenuation of the source laser light at NIR ranges propagating through the soft tissues, and an optimal design of the light source and energy delivery method is pivotal for the deep tissue PA imaging [16-18].

PAI technique can mainly be used for breast tumor detection because of the high contrast between the breast tissue and the tumor, because of the limited penetration depth of laser radiation, and the well projection of the breast organ outside the human body.

Experimental procedure

Photoacoustic experiments were performed using an arrangement which consists of a light source, piezoelectric detector, and data-acquisition system. The arrangement used to perform photoacoustic measurements in vitro on different phantoms is shown in figure 2. Q-switched Nd:YAG laser has been used to irradiate the phantoms, which generates light pulses with a duration of 10 ns, and a repetition rate of 1 Hz. The pulse duration fulfills the requirements of stress confinement for generating photoacoustic signal. The phantoms were irradiated using near-infrared and visible

wavelength range of 1064 nm and 532 nm respectively. The laser pulse energy was 445mJ.

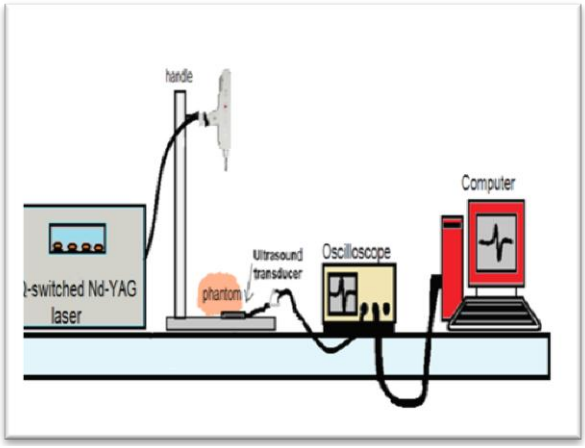

Fig. (2): Schematic picture of the experimental arrangement

More than 30 phantoms in different arrangements have been tested, 11 of which are presented in this work as distinctly significant results. These phantoms have been prepared with two types of object:

Biological tissue: fish heart 1to8mm in diameter as shown in figure 3. It was difficult to obtain signal from fish heart with low noise due to the porosity and cavities in the fish heart organ. Fish heart loses its blood content in few hours where it becomes difficult to obtain any signal; therefore it is recharged with blood.

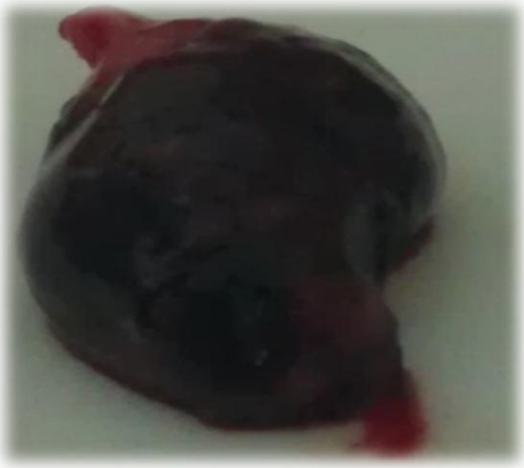

Fig. (3): Fish heart organ

Blood sac: which is made from silicon rubber charged with blood, with a diameter ranging between 5 and 14mm as shown in figure 4. The signals obtained from this type were noise-free due to the absence of porosities.

Fig. (4): Blood sac

However these phantoms cannot be used after a while, because the Red blood cell viability decrease during storage as a result of physical and metabolic changes, increase temperature (exceed 6°C) speed up the damage of the red cell (hemoglobin is dissociated into heme and globin) [19]. These objects were embedded in chicken breast tissue, or placed on the upper surface of the tissue, as single or dual object. The thickness of chicken breast tissue ranged between 3 and 21mm.

These phantoms need to have optical and acoustical properties corresponding to the real tissue [20]. Because of the absorption contrast (α_{object} & α_{tissue}) between the fish heart organ or blood sac and chicken breast (chicken breast has approximately the same optical absorption to the human breast tissue [21] therefore they have been used as phantoms, as shown in figure5.

Fig. (5): The phantom (2 pieces of chicken breast issue and fish heart as a tumor)

The signals from these phantoms were detected by piezoelectric detector. Lenses with focal length of 2.5, 7.5 and20cm were used for expanding laser spot to fulfill the spherical model requirment, covering the whole object with the laser radiation.

Finally these signals and corresponding data were recorded by digital storage oscilloscope and imaged in a microcomputer using matlab software.

Experimental Results

The following parameters have been measured in this work

Object diameter evaluation

In time domain positive and negative peaks, can be used to determine the object diameter, If the sound speed c in the object is known, then time from peak to can be used to determine the object diameter [22-24], using the equation:

$$d = c\,(t_2 - t_1)$$

Where t_1 is the recorded time of the positive pressure peak and t_2 is the time of the negative pressure peak. This evaluation has been done with two types of objects:

Results of using fish heart organ

Phantoms with object size 5, 6, 7 and 8mm has been irradiated with 445mJ, gave the signals shown in figure 6.

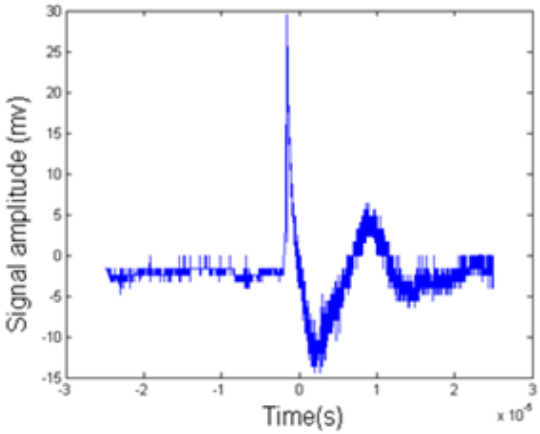

(a)

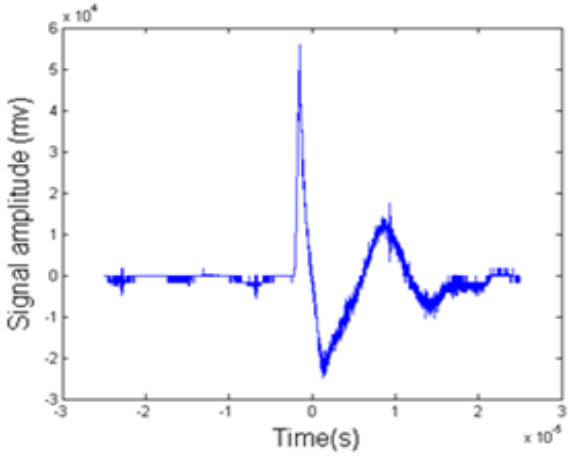

(b)

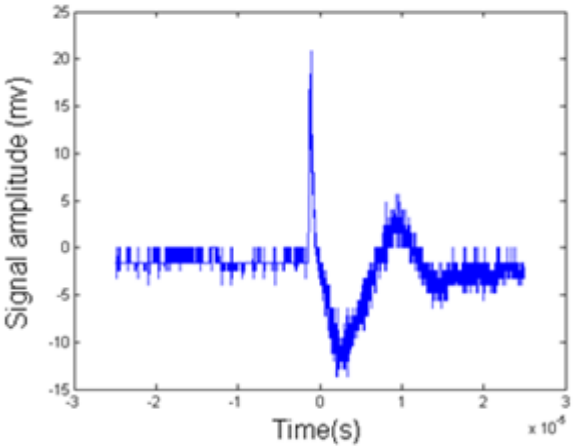

(d)

Fig. (6): Signals of different objects size (a) 5mm (b) 6mm (c) 7mm and (d) 8mm

The results of the fish heart organ from the signals in figure 9 gave the following results in table 1

Table (1): Diameter of fish heart organ measurements

Real diameters (mm)	Measured diameters (mm)
5	5
6	5.7
7	7.3
8	7.7

Results of using a blood sac

Phantoms with object size 14, 13 and 5mm has been irradiated with 445mJ, gave the signals shown in figure 7.

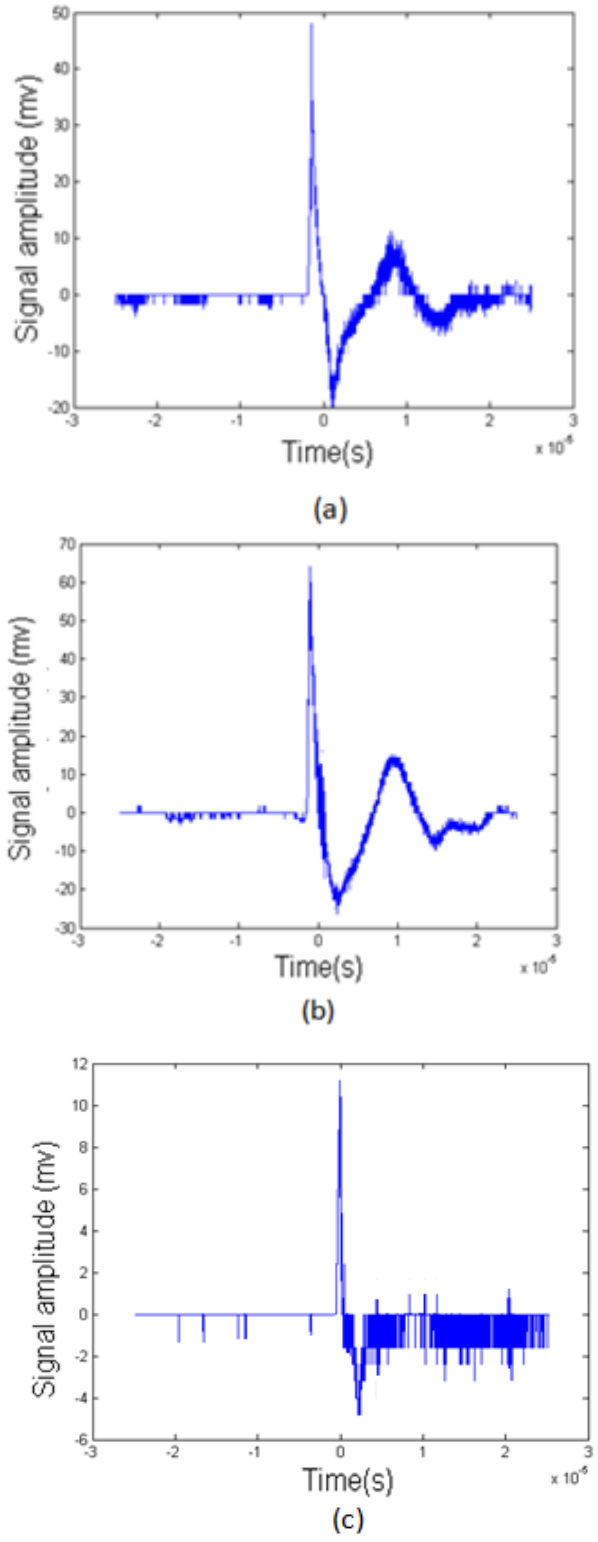

Fig. (7): Signals of different objects size (a) 14mm (b) 13mm(c) 5mm

The results of the blood sac from signals in figure 7 gave the following results in table 2

Table (2): Diameter of blood sac measurements

Real diameters (mm)	Measured diameters (mm)
14	7.1
13	6.8
5	4.6

The signal results from figures 6 and 7 shows that the signal from the blood sac is cleaner and easier to be generated from the object because the sac is filled with blood, however the porosity in the fish heart organ helps to give a signal with better results (object size) because it fulfills the spherical model due to its low absorption ability compared with blood sac. Blood sac of 5mm diameter can be measured easier and more correct than larger one.

Effect of the detector position

Phantom with object size 7mm has been irradiated with 445mJ and the signal has been detected in different piezoelectric positions, the resulting signal as shown in figure 8.

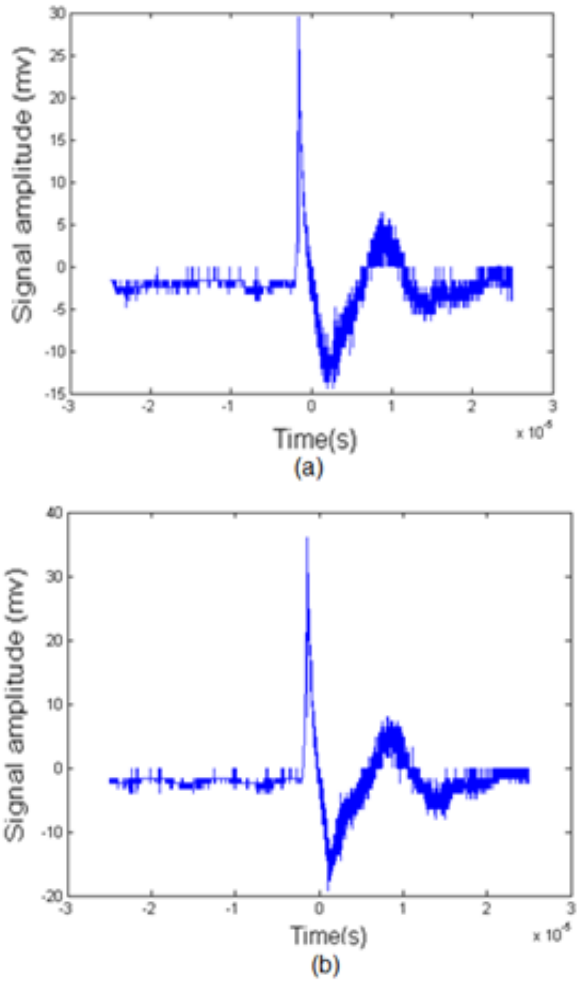

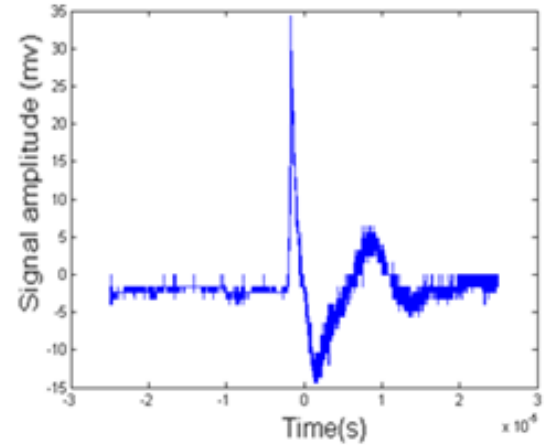

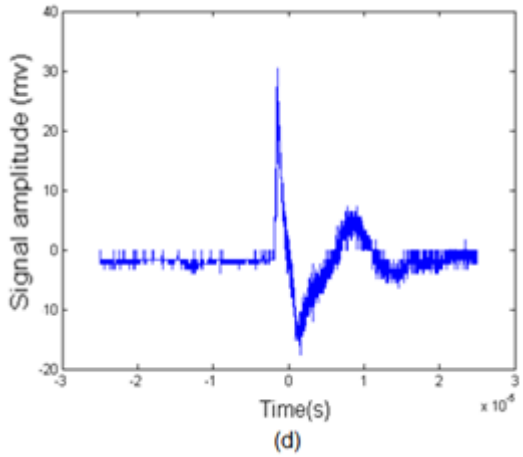

Fig. (8): Signals with different piezo positions (***i).*** beneath phantom (b) beneath phantom, 60 mm off the object centre (c) beneath phantom, 110 mm off the object centre (d) beneath phantom, 120 mm off the object centre

The results from the signals in figure 8 from object with diameter 7mm gave the following results in table 3.

Table (3) Diameter of different piezoelectric detector positions

Piezo detector positions	Measured diameters (mm)
beneath phantom	7
beneath phantom, 60 mm off the object centre	6
beneath phantom, 110 mm off the object centre	5.3
beneath phantom, 120 mm off the object centre	5.2

The image will be seen from these signals is shown in figure 9.

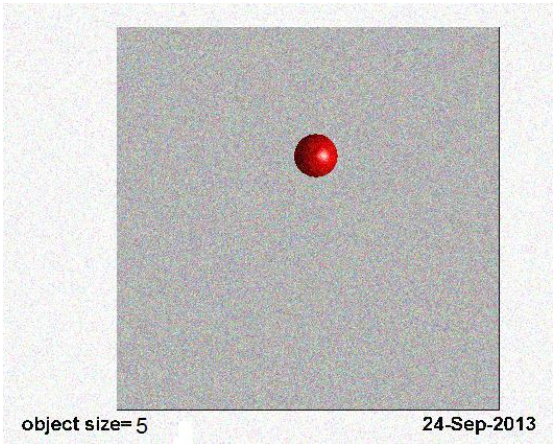

Fig. (9): Image of phantom with one object

The results from signals in figure 8 shows that the acoustic signal can be detected even if the detector far away from the object (tumor) up to 120 mm, however the rate of error was increased with the increase of the distance, because of signal attenuation.

Measurement of distance between two objects

Phantom with two objects has been used to measure 1-4mm distance between the objects. Figures 10 and figure 11 presented the signal results when different wavelengths were used with diffusion lens of focal length 2.5cm for measuring these different separating distant.

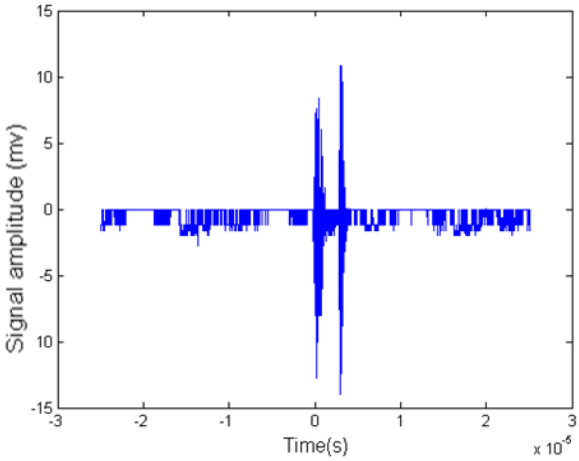

Fig. (10): PA signals when 532nm used with 2.5cm diffusion lens

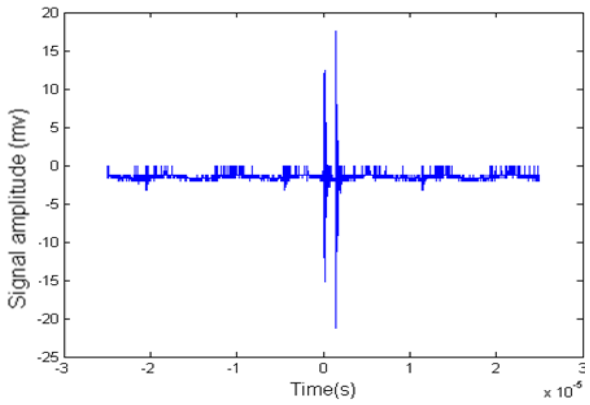

Fig. (11): PA signals when 1064nm used with 2.5cm diffusion lens

The resulting distance between the two objects was 4.3mm for 532nm and 2.5mm for 1064nm.The image from these signals as shown in figure 12.

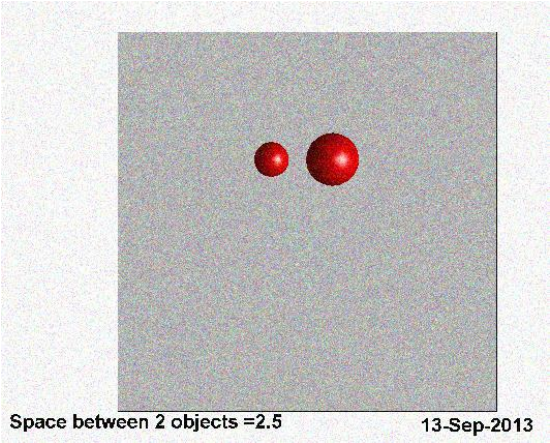

Fig. (12): Image of phantom with two objects

Results from the figures 10 and 11 shows that the signal obtained from wavelength 1064nm was more distinctive compared with signal obtained from 532nm, due to the peak blood adsorption in the visible range resulting in higher noise due to the contrast between the blood and the porosity of the fish heart tissue.

The object size can't be obtained from these signals because the diameter measured is restricted by the absorption depth. Low energy density causes low absorption depth therefore the diameter measured is so small compared with the real diameter.

Conclusions

From the experiments that have been accomplished and analyzed, the following conclusions have been deduced:

1. The peak-to peak time (τ_{pp}) of the laser induced pressure wave has been used to estimate the object diameter (or axial dimension). The measurement analysis shows that the estimated object dimension is significantly dependent upon object absorptivity and laser energy density. The error in fish heart object dimension ranged from -14% to +9%. The Maximum error in Blood sac object dimension was -55%. While object dimension error increased to -92% when the laser spot was magnified from 2mm to 45mm (to cover the phantom area) as the energy density decreases significantly.
2. The pressure amplitude of the signal was linearly proportional with the laser pulse energy according to Beer lambert law, and inversely proportional with the depth of target object and the distance from the object to the detector due to signal attenuation.
3. The blood must exist in fresh form to obtain the right results. Red blood cell viability decrease during storage and with increase in temperature. It's found that when the blood damaged, no signal can be detected, while fresh blood gives. It's expected that a shift in an absorption line has occurred that why no signal could be received. So the blood was replaced by a fresh one injected in the object.
4. The signal obtained from wavelength 1064nm was more distinctive compared with signal obtained from 532nm, due to the peak blood adsorption in the visible range resulting in higher noise due to the contrast between the blood and the tissue (porosity).

References

A. Briggs, and O. Kolosov, "Acoustic microscopy", Oxford University Press, 2nd Ed.

And Perfusion In Tissue, (2002), "PhD thesis, University of Twente.

Ben Cox ; Jan G. Laufer et al, (2008)" Ultrasound and photoacoustic imaging to guide and monitor photothermal therapy", Ph.D. Dissertation, Texas at Austin university.

Chengyi yan, (2009), ”Energy storage in chlamydomonas reinhardtii measured with photoacoustic techniques”, M.SC thesis, University of New Jersey X.

Craig B. Sussman, Candace Rossignol1et al, (2012), ”Photoacoustic tomography can detect cerebral hemodynamic alterations in a

neonatal rodent model of hypoxia-ischemia", society for neuroscience journal, Acta Neurobiol **72**, 253–263.

D. J. Weiss DVM and Jane K. Wardrop, PhD, DACVP, (2010), " Schalm s veterinary hematology", Wiley-Balckwell, 6th Ed.

Eric Strohm et al., (2012), "Photoacoustic spectral characterization of perfluorocarbon droplets", SPIE journal **8223**, 82232.

Etienne De Montigny, (2011), " Photoacoustic tomography principles and applications", Department of Physics Engineering, polytechnic school Montreal.

Geng Ku, (2004), "Photoacoustic and Thermoacoustic Tomography System Development For Biomedical Applications", PhD Dissertation, Huazhong University of Science and Technology.

Israa Safaa Al- Zubaidy, (2008), "Study of breast tumor diagnosis using optoacoustic technology", MSC Thesis, Nahrain University.

J. Biomed., (2012), " Quantitative spectroscopic photoacoustic imaging: a review", Journal of Biomedical Optics ,**17** ,6 .

Jason Zalev, (2010), " Detection and monitoring for cancer and abnormal vasculature by photoacoustic signal characterization of structural morphology", M.Sc. thesis, Ryerson University.

John Andrew Viator, (2000), " Characterization of photoacoustic sources in tissue using time domain measurements",Ph.D. thesis , Oregon University.

L. Fieramonti, (2010), "Feasibility, development and characterization of a photoacoustic microscopy system for biomedical applications", M.Sc thesis, Lund University.

Lihong V. Wang,et al., (2012), "Organs photoacoustic tomography: in vivo imaging from organelles to orangs", science AAAS journal, **335**, 1458-1462.

Luca Fieramonti, (2010), "Feasibility, development and characterization of a photoacoustic microscopy system for biomedical applications", M.Sc thesis, Lund University X.

P. Luke, (2012), "Biomedical applications of photoacoustic imaging wit exogenous contrast agents", BMES biomedical engineering society journal, **40**, 2, 422-437.

R. G. M. Kolkman, (2006), "In vivo photoacoustic imaging of blood vessels with a pulsed laser diode", lasers medical science journal, **21**, 134-139.

R.G.M. Kolkman.," Photoacoustic & Pulsed Laser-Doppler Monitoring Of Blood Concentratio

Rui Ma, Adrian Taruttis et al, (2009), "Multispectral optoacoustic tomography (msot) scanner for whole-body small animal imaging", optics express journal ,**17**, 24 , 21414- 21426.

Sung-Liang Chen, (2012), " Optical microring resonators for photoacoustic imaging and detection", PhD dissertation, Michigan university.

Wang, Y Pang, et.al., (2003), "Noninvasive laser- induce photoacoustic tomography for structural and functional in vivo imaging of the brain", nature biotechnology journal, **21**, 7, 803-806.

Xin Cai, (2013), "Photoacoustic microscopy in tissue engineering", Elsevier journal, **16**, 3.

Yao Sun et al., (2011), "Photoacoustic imaging: an emerging optical modality in diagnostic and theranostic medicine", Biosensors & Bioelectronics journal , **2** , 108.

Zhaohui Wang, Seunghan Ha, et al., (2012), " A new design of light illumination scheme for deep tissue photoacoustic imaging", optical society of america journal, **20** , 20.

التصوير الضوئي-الصوتي للانسجة الحية للتطبيقات الطب الاحيائي

اروى عامر موسى محمد عبد الامير حسين

قسم هندسة الليزر والالكترونيات البصرية ، جامعة النهرين ، بغداد ، العراق

الخلاصة: التصوير الضوئي-الصوتي هو أسلوب التصويرالفريد الذي يجمع تباين امتصاص الضوء او تردد الموجات الراديوية مع شدة الموجات فوق الصوتية. فعند إختزان الطاقه الضوئية خلال مدة زمنيه قصيرة، سيتولد تمدد حراري مرن والذي يولد بدوره الموجات الصوتيه. ممكن ان تسجل وتخزن هذه الموجات لبناء الصورة . يقدم هذا العمل مساقات تجريبية باستخدام الليزرللتصوير ثنائي الابعاد للكشف عن الورم السرطاني الموجود داخل الانسجه الطبيعية. تم انجاز التجارب العملية بااستخدام عينات شبحية تتكون من قلب السمك او كيس دم (لمحاكاة الورم) معدل قطرها 1-14 ملم مطمورة داخل قطعة من صدر الدجاج، وذلك لتشبيه النسيج الحقيقي. وقد تم استخدام ليزر النديميوم-ياك بطول موجي 1.064 مايكرو متر وطول نبضة 10 نانو وطاقة 445 ملي جول للحصول على اشارة الموجة الصوتية في هذه الاهداف المختلفه. ثم تمت تنقية وتحليل الاشارة الصوتية لبناء صورة الهدف. وقد تم تحليل البيانات العمليه وبناء الصور باستخدام برامجية matlab. اظهر تحليل القياسات تطابقا معقولا حجم الجسم المقدر وحجمه الحقيقي. تراوحت نسبة الخطأ في ابعاد جسم قلب السمكة -14% الى + 9%. في حين كانت اكبرنسبة خطأ في ابعاد جسم كيس الدم -55%. وقد ارتفعت نسبة الخطأ في ابعاد الجسم الى -92% عند تكبير بقعة الليزر من 2مليم الى 45 مليم (لتغطية مساحة الشبح) والتي ادت الى تقليل كثافة الطاقه بشكل كبير.